

PACS numbers: 42.65.Jx; 42.65.Re; 52.50.Jm
DOI: 10.1070/QE2014v044n06ABEH015452

Plasma channels in a filament of a femtosecond laser pulse focused by an axicon

S.V. Chekalin, A.E. Dokukina, E.O. Smetanina, V.O. Kompanets, V.P. Kandidov

Abstract. **We report the results of experimental and numerical investigation of the influence of the wavefront curvature of femtosecond light focused by an axicon on the length and position of plasma channels in the filament under conditions of normal and anomalous group velocity dispersion in fused silica. It is shown that a change in the wavefront curvature by a value much greater than the longitudinal dimensions of the filament noticeably changes the geometry of the plasma channel position. The role of axicon focusing for ordering multiple filamentation is studied experimentally.**

Keywords: *filamentation, femtosecond pulses, anomalous dispersion, plasma channels, light bullets.*

1. Introduction

Bessel beams attract researchers' attention as beams having a transverse intensity distribution at which the diffraction divergence is absent in the case of an infinite aperture [1]. Such beams make it possible to design optical manipulators, atomic guides in atomic physics and other unexpected applications [2]. Bessel beams are usually generated by using an axicon forming a conical wavefront from a plane wavefront [3]. In focusing a Gaussian beam by an axicon, a beam with a Bessel–Gaussian profile is formed, the diffraction divergence of which is determined by the aperture of the beam incident on the axicon. The length of the localisation region of the axicon-generated beam exceeds the waist length of the beam focused by a spherical lens. This property of Bessel–Gaussian beams allows extended plasma channels to be formed when nanosecond laser pulses propagate in air [3]. Axicon focusing of subterawatt femtosecond pulses into a transparent dielectric target was used in [4] to increase the length of the nonlinear optical interaction of radiation with the medium.

Axicon focusing of femtosecond laser beams significantly affects filamentation of light. The regimes of formation of a single filament, when a Gaussian beam is focused by an axicon with different angles of beam convergence, were investigated theoretically by Polesana et al. [5]. In pulses, the power of which is dozens of times greater than the critical self-focusing power, the use of axicon focusing can suppress and regularise stochastic multiple filamentation during which an array of randomly arranged filaments with a high power density is produced [6]. As a result, instead of a speckle pattern, in the conical emission during multiple filamentation formed under conditions of lens focusing, a regular system of concentric rings is produced. The authors of paper [7] obtained a cylindrically symmetric ordered set of filaments in a methanol solution when a 50-fs pulsed beam at $\lambda = 800$ nm was focused by an axicon. Under tight axicon focusing of a Gaussian beam the intensity in the filament and the electron density in the plasma channel increase significantly [8].

Of greatest interest is an increase in the length of plasma channels in a filament through focusing laser light by an axicon as compared to focusing by a spherical lens. According to the numerical study [9], when a Gaussian beam is focused by an axicon, there emerges an elongated narrow plasma channel with a uniformly distributed electron density, which is unattainable in using a spherical lens. In experiments on filamentation of 1.055-μm, 1-ps axicon-focused laser pulses in a solution of Coumarin in methanol, Polesana et al. [10] detected plasma channels a few centimetres in length, in contrast to the millimetre-long channels observed in experiments with lens focusing. The authors of [11, 12] found the length of plasma channels to be four-to-ten times longer in the case of axicon focusing as compared to lens focusing during filamentation of laser pulses with a duration of 50–150 fs at $\lambda = 800$ nm in air. Using divergent axicon-focused Gaussian beams allowed a triple increase in the length of the plasma channel during filamentation of 500-fs pulses at a wavelength of 248 nm in air [13].

In this paper we study the effect of the wavefront curvature of a femtosecond axicon-focused Gaussian beam and material dispersion of fused silica on the formation of plasma channels. We present the results of experimental and numerical studies of plasma generation in fused silica during filamentation of 800- and 1800-nm pulses, which lie in the region of normal and anomalous group velocity dispersions, respectively.

2. Methods of experimental and numerical study

Plasma channels produced in the process of femtosecond filamentation of Bessel–Gaussian laser beams at $\lambda = 1800$ and 800 nm in fused silica were studied experimentally by using a spectroscopic stand from the Centre of Joint Research at the Institute of Spectroscopy, RAS [14]. The setup consisted of a femtosecond tunable TOPAS parametric amplifier combined

S.V. Chekalin, V.O. Kompanets Institute of Spectroscopy, Russian Academy of Sciences, ul. Fizicheskaya 5, 142190 Troitsk, Moscow, Russia; e-mail: chekalin@isan.troitsk.ru, kompanetsvo@isan.troitsk.ru;
A.E. Dokukina, E.O. Smetanina, V.P. Kandidov Department of Physics, M.V. Lomonosov Moscow State University, Vorob'evy gory, 119991 Moscow, Russia; e-mail: smetanina@physics.msu.ru, spirkov@physics.msu.ru, kandidov@physics.msu.ru

Received 3 March 2014; revision received 24 March 2014
Kvantovaya Elektronika **44** (6) 570–576 (2014)
Translated by I.A. Ulitkin

with a regenerative Spitfire Pro amplifier. Pulses from a femtosecond Tsunami (Ti:sapphire) laser pumped by a cw solid-state Millenia Vs laser were fed to the regenerative amplifier pumped by a solid-state Empower 30 laser. From the amplifier's output femtosecond laser light with a close-to-Gaussian transverse intensity profile was coupled to the telescope made of two thin quartz lenses which made it possible to change the transverse beam size and radius of curvature of its wavefront (Fig. 1). The telescope-generated beam was incident on a flat face of a quartz axicon with a cone angle of 179°. The radius of the spot on the flat face of the axicon after telescopic system was 1 and 0.9 mm for light at $\lambda = 1800$ and 800 nm, respectively. The axicon tip touched the entrance face of the sample made of fused silica, and thus the formation of a Bessel intensity distribution in the cross section of the femtosecond Gaussian beam occurred simultaneously with its transformation in the process of self-action in the fused silica sample. Recombination emission from the laser plasma in the filament and its conical emission in the sample were recorded with a digital camera through the side face of the sample, which made it possible to determine the length and position of plasma channels and evaluate the density of electrons by the brightness of the filaments, thereby obtaining information about localisation of the regions with the highest optical field intensity in the filament. To avoid an irreversible change in the refractive index of the material, the fused silica sample was moved regularly in the cross section of the laser beam.

In the experiment at $\lambda = 800$ and 1800 nm we used pulsed radiation of duration $\tau_{FWHM} = 50$ fs. The pulse energy was varied from 3 to 105 μJ, and the repetition rate was 1 kHz.

In studying numerically the filamentation of femtosecond Bessel–Gaussian beams we used a slowly varying wave approximation. The system of equations for the complex field amplitude and the electron density in fused silica included the wave effects of diffraction, dispersion, pulse envelope wavefront self-steepening, Kerr nonlinearity with a contribution of the Raman response of the medium taken into accont, generation of electrons due to photoionisation and avalanche ionisation in a strong laser field, defocusing and absorption in an induced laser plasma [15]. The group-velocity dispersion was described by the Sellmeier equation and the photoionisation rate – by the Keldysh formula. The complex field amplitude $A(r,\tau,z)$ at the input plane of the fused silica sample ($z = 0$) had the form:

$$A(r,\tau,z=0) = A_0 \exp\left[-\frac{r^2}{2w_0^2} - \frac{\tau^2}{2\tau_0^2} + \mathrm{i}\frac{k_0 r^2}{2R} + \mathrm{i}\varphi_{ax}(r)\right], \quad (1)$$

where w_0 and τ_0 are the beam radius and the half-width pulse duration at the e^{-1} level; R is the radius of the wavefront curvature of the beam impinging on the axicon (varied by changing the distance between the telescope lenses); k_0 is the wave number; $\varphi_{ax}(r) = kr\beta$ is the phase shift of radiation in the axicon; $\beta = (n_{ax} - 1)\alpha/n_{sil}$ is the beam convergence angle in fused silica after axicon focusing; $\alpha = 0.5°$ is the angle at the base of the axicon; and n_{ax} and n_{sil} are the refractive indices of the axicon material and fused silica sample, which were taken equal to 1.44. Expression (1) did not take into account the nonlinear phase shift during propagation of radiation in the optical elements of the telescope and axicon because the total thickness of these elements did not exceed 0.5 cm, whereas, according to experimental data, a filament is formed at a distance of 4–5 cm from the entrance face of the sample.

The numerical solution of the self-consistent system of equations for the field amplitude $A(r,\tau,z)$ and the electron density $N_e(r,\tau,z)$ in the induced laser plasma made it possible to determine the change in the electron density on the axis of the plasma channel, $\tilde{N}_e(z)$, along the filament after the termination of the pulse.

3. Similarity parameters

Formation of plasma channels in a femtosecond filament depends on a set of medium and radiation parameters. At the

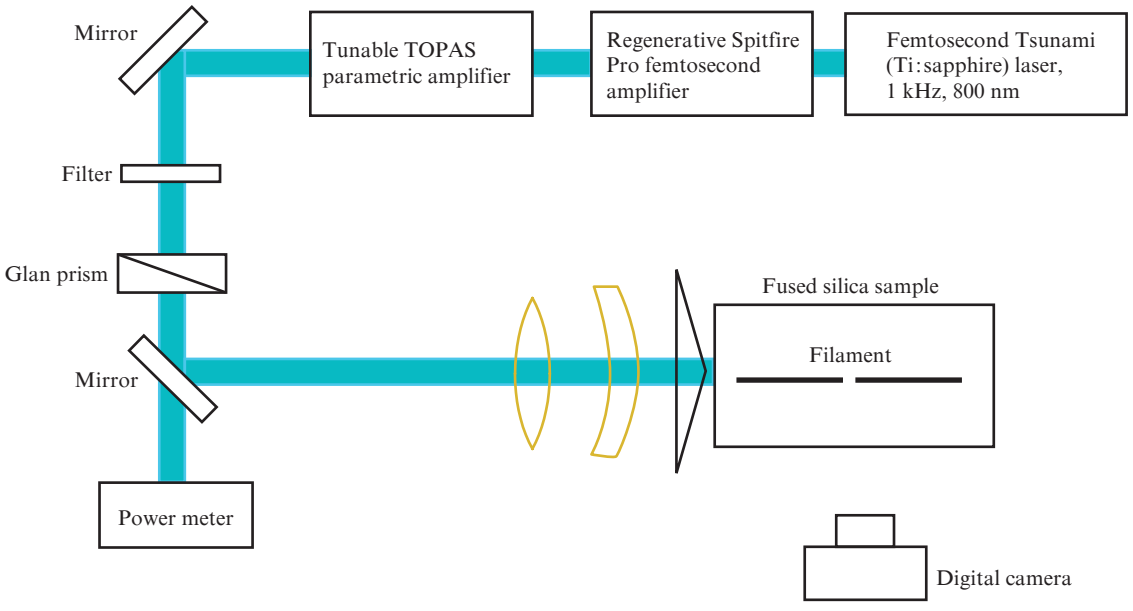

Figure 1. Schematic of the experimental setup.

Table 1.

λ/nm	k_2/fs^2 cm^{-1}	n_2/cm^2 W^{-1}	P_{cr}/MW	K	b_0/mm	L_{diffr}/cm	L_{disp}/cm	Z_{Bess}/cm
800	360	3×10^{-16}	2.2	6	0.12	3.3	2.4	~30
1800	–625	3×10^{-16}	11.2	14	0.26	5.9	1.4	~30

Note: Radius of the central lobe b_0 of the Bessel–Gaussian distribution is determined by zeroing the intensity in the plane of the beam cross section; Z_{Bess} is the length at which the peak intensity of the central lobe reaches a maximum value; and L_{diffr} is given for the central lobe.

initial stage of the filamentation process, before the formation of plasma channels and defocusing of the beam, the spatio-temporal evolution of the optical field in the induced laser plasma is determined by dispersion, diffraction and Kerr self-focusing of radiation. The dispersion length L_{disp}, diffraction length L_{diffr} and the filament start distance L_{fil} are thus the similarity criteria for the initial stage of the filamentation of laser pulses with different wavelengths. In fused silica the parameter $k_2 = (\partial^2 k/\partial\omega^2)_{\omega_0}$ determining the dispersion spreading of a pulse is positive, which corresponds to the normal group-velocity dispersion, and equals 360 fs^2 cm^{-1} at λ = 800 nm, and at λ = 1800 nm $k_2 = -625$ fs^2 cm^{-1} and the group velocity dispersion is anomalous. For the considered pulses with τ_{FWHM} = 50 fs, the dispersion length is L_{disp} = 2.4 and 1.4 cm at λ = 800 and 1800 nm, respectively.

For beams with a Bessel–Gaussian intensity distribution the filament arises as a result of self-focusing on the axis of the beam. Therefore, the similarity parameters at the initial stage of filamentation are diffraction (L_{diffr}) and nonlinear (L_{fil}) lengths defined for the central lobe in the Bessel–Gaussian beam.

The diffraction length L_{diffr} of the central lobe of the Bessel–Gaussian beam is determined by the lobe radius and laser wavelength. The central spot size depends only on the laser wavelength and the beam convergence angle β [3]. In these conditions, the radius of the central lobe, measured by the distance from the axis to the first zero in the intensity distribution in the beam cross sectional plane, is 265 μm at λ = 1800 nm and 118 μm at λ = 800 nm. By approximating the central lobe of the Bessel–Gaussian distribution by a Gaussian beam with a radius equal to the radius of the central lobe at the e^{-1} level, we obtain L_{diffr} = 3.3 and 5.9 cm at λ = 800 and 1800 nm, respectively.

The main parameters determining the nonlinear length L_{fil}, which gives rise to a filament for a beam with a Bessel–Gaussian intensity distribution, are the nonlinearity parameter n_2 and the power contained in the central lobe. Assuming that at 800 and 1800 nm, the nonlinearity parameter in fused silica is $n_2 \approx 3.0\times10^{-16}$ cm^2 W^{-1}, we obtain the following estimates: A critical self-focusing power in fused silica, P_{cr}, at λ = 800 and 1800 nm is 2.2 and 11.2 MW, respectively. The numerical study of the formation of a Bessel–Gaussian profile in the case of axicon focusing of a Gaussian beam in the absence of material dispersion and nonlinearity showed that in the Bessel–Gaussian profile formed, the central lobe, when reaching a maximum intensity, contains 23% of Gaussian beam power at λ = 800 nm and 55% of power at λ = 1800 nm. For the parameters considered, the distance Z_{Bess} is ~30 cm, at which, in the absence of material dispersion and nonlinear interaction with the medium, the intensity of the central lobe of the Bessel–Gaussian distribution reaches a maximum. Assuming that the central lobe has a Gaussian profile of the transverse intensity distribution, the Marburger–Talanov formula [16] can be used to estimate the filament start distance L_{fil}. At λ = 800 nm with pulse energies 7, 18 and 41 μJ the length L_{fil} is 0.65, 0.36 and 0.23 cm, respectively, and at λ = 1800 nm with pulse energies 22, 36 and 105 μJ the length is 1.3, 0.9 and 0.5 cm, respectively.

It should be noted that in this scheme (see Fig. 1) filamentation in fused silica occurs in a dispersive medium during the formation of a Bessel–Gaussian intensity distribution at different wavefront curvatures of the beam incident on the axicon. While the estimates of the similarity parameters are conditional, they are convenient for a comparative analysis of filamentation regimes at different pulse parameters. Interaction of radiation with the generated plasma is characterised by a number of parameters, the most important of which is the order of the multiphoton ionisation process, K. The parameters describing the propagation of radiation in fused silica are shown in Table 1, and the similarity parameters to the problem of filamentation of a beam focused by an axicon at different wavelengths and energies – in Table 2.

Table 2.

E/μJ	λ/nm	Similarity parameters	
		P/P_{cr}	L_{fil}/cm
7	800	60 (14)	0.65
	1800	–	–
18	800	154 (35)	0.36
	1800	–	–
22	800	–	–
	1800	37 (20)	1.3
36	800	–	–
	1800	60 (33)	0.9
41	800	350 (80)	0.23
	1800	–	–
105	800	–	–
	1800	175 (96)	0.5

Note: The nonlinear length L_{fil} is given for the central lobe, and the ratio P/P_{cr} – for a Gaussian beam incident on the axicon and the central lobe of the Bessel–Gaussian distribution (in parentheses).

4. Plasma channels

The photographs of plasma channels, detected by the plasma recombination luminescence, and supercontinuum radiation scattered in fused silica during its propagation along the filament are shown in Fig. 2. Black-and-white images have dark and gray areas corresponding to the red glow of the plasma and to scattered radiation in the visible band of the supercontinuum. Due to the scattering in fused silica, the supercontinuum intensity decreases with distance from the region of its generation, which coincides with the plasma

channel. One can see that in comparison with the case of a collimated beam, the distance before the filament start (regardless of the wavelength) decreases in the case of axicon focusing of a beam with a converging wavefront and increases in the case of focusing of a beam with a diverging wavefront. Note that the filament start distances are close at both wavelengths, despite the fact that the excess of the peak self-focusing power in the central lobe of the Bessel–Gaussian beam over the critical power at $\lambda = 800$ nm is significantly higher than at $\lambda = 1800$ nm. This is due to a strong influence of dispersion on the filament formation at $\lambda = 800$ nm, since the dispersion length is two-to-three times less than the distance from the filament start, observed in the experiment (Table 1, Fig. 2). During filamentation at $\lambda = 800$ nm, i.e., under conditions of normal group-velocity dispersion, the peak power continuously decreases, because such dispersion leads to its spreading. In the process of filamentation at $\lambda = 1800$ nm, as a result of the joint effect of the Kerr self-phase modulation and anomalous group-velocity dispersion the pulse compresses because the optical field from the outer temporal slices catches up with the central. Thus, at $\lambda = 800$ nm the peak laser power is significantly reduced due to the dispersion, and at $\lambda = 1800$ nm – increases, thereby increasing the number of plasma channels in the filament at the same excess of the power over the critical. Therefore, the excess of the power over a critical value, taking place for radiation at $\lambda = 800$ nm, is excluded from the nonlinear interaction which leads to an increase in the filament start distance and to a decrease in the number of plasma channels.

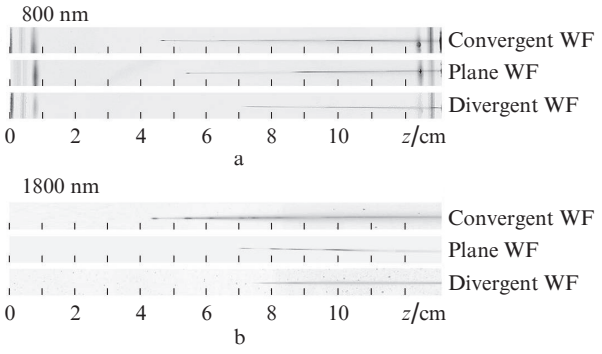

Figure 2. Experimentally recorded filament glow at different energies, wavelengths and wavefront geometries of radiation focused by an axicon [radius of curvature of beams with convergent and divergent wavefronts (WFs) is $R \approx 3$ m]: (a) beam with an energy 18.5 μJ at $\lambda = 800$ nm (normal group-velocity dispersion); (b) beam with an energy 22 μJ at $\lambda = 1800$ nm (anomalous group-velocity dispersion).

A chain of plasma channels along the filament, clearly detected for converging and collimated beams, is the result of increasing intensity during refocusing of the central lobe of the Bessel–Gaussian beam, whose power far exceeds the critical self-focusing power (see Fig. 2). In the region of each plasma channel, where the intensity in the filament is maximal, a supercontinuum is generated, which is detected by an increase in the scattered radiation intensity after each channel [15]. Away from the generation region, the supercontinuum intensity due to scattering in fused silica decreases. As follows from the experiment, the short-wavelength component in the visible region of the spectrum is more intense during filamentation at $\lambda = 1800$ nm than at $\lambda = 800$ nm. The difference in the supercontinuum spectra at different wavelengths is explained by the difference in the orders of the multiphoton ionisation process. At $\lambda = 1800$ nm the order of multiphoton ionisation is higher than at $\lambda = 800$ nm, and, as a result, the steepening of the trailing edge of the pulse in this case is more important; therefore, the supercontinuum spectrum is more shifted to the anti-Stokes region [17]. In the experiment, the brightest plasma glow, corresponding to the highest electron density, is observed in beams with convergent and flat wavefronts, despite the fact that the radius of the wavefront curvature R is many times greater than the longitudinal scales of transformation of radiation.

A sequence of plasma channels, obtained by simulating numerically the filamentation of pulses at different wavelengths and the same excess of the peak power over a critical value is presented in Fig. 3. At $\lambda = 800$ nm, as in the experiment, visible is a sequence of localised plasma channels with a longitudinal size of about 1 mm, which are spaced apart by a distance of ~2 cm. Figure 3a shows the distribution of the free carrier density $N_e(r, z)$ in the filament cross section as a function of distance to the axicon. It can be seen that the plasma channels consist of two local maxima of plasma concentration. This is due to the fact that under conditions of normal dispersion and Kerr self-phase modulation, the pulse splits into subpulses, each of which generates laser plasma. For example, the first channel in Fig. 3a has a pedestal with a low plasma density and a narrow peak with a high plasma density. As the analysis of the spatiotemporal pulse shape evolution shows, the pedestal is generated by a subpulse, departed to the pulse front, and the narrow peak is generated by a subpulse located on the tail of the pulse. Plasma in the subpulses is generated simultaneously, but the concentration maximum in the front subpulse is achieved at a smaller distance than in the latter case. Since the peak intensities in the subpulses do not coincide, the local maxima of the electron density are different. The local minimum of the electron density on the axis $N_e(r = 0, z)$ corresponds to a decrease in the intensity of subpulses during their transformation with distance. The second plasma channel shown in Fig. 3a has the same structure as the first one; however, the maximum with a low electron density precedes here a sharp peak with a high density. In this case, the pedestal is generated by a subpulse, departed to the pulse front. The local minimum in the plasma channel occurs at the time of the splitting of the front subpulse into another two subpulses, i.e., the pulse at this point is split into three subpulses, and the second of which gives rise to a sharp peak in the second plasma channel. Thus, the longitudinal plasma distribution in a channel under conditions of normal group-velocity dispersion is dependent on the pulse time dynamics, i.e., on such parameters as the number of the subpulses, into which the pulse is split, and on the peak intensity and duration of subpulses.

Under conditions of anomalous group-velocity dispersion at $\lambda = 1800$ nm plasma channels also have a length of ~ 1 mm, but spaced apart by a distance of about 5 mm. Note that at the same excess of the power over a critical value, P/P_{cr}, the number of plasma channels in the case of the axicon focusing of collimated light at $\lambda = 1800$ nm (Fig. 3c) is much greater than when the light is focused at $\lambda = 800$ nm (Fig. 3a).

When a divergent beam at $\lambda = 1800$ nm is focused by an axicon (Fig. 3d), the distance to the first plasma channel is greater than in the case of axicon focusing of a collimated

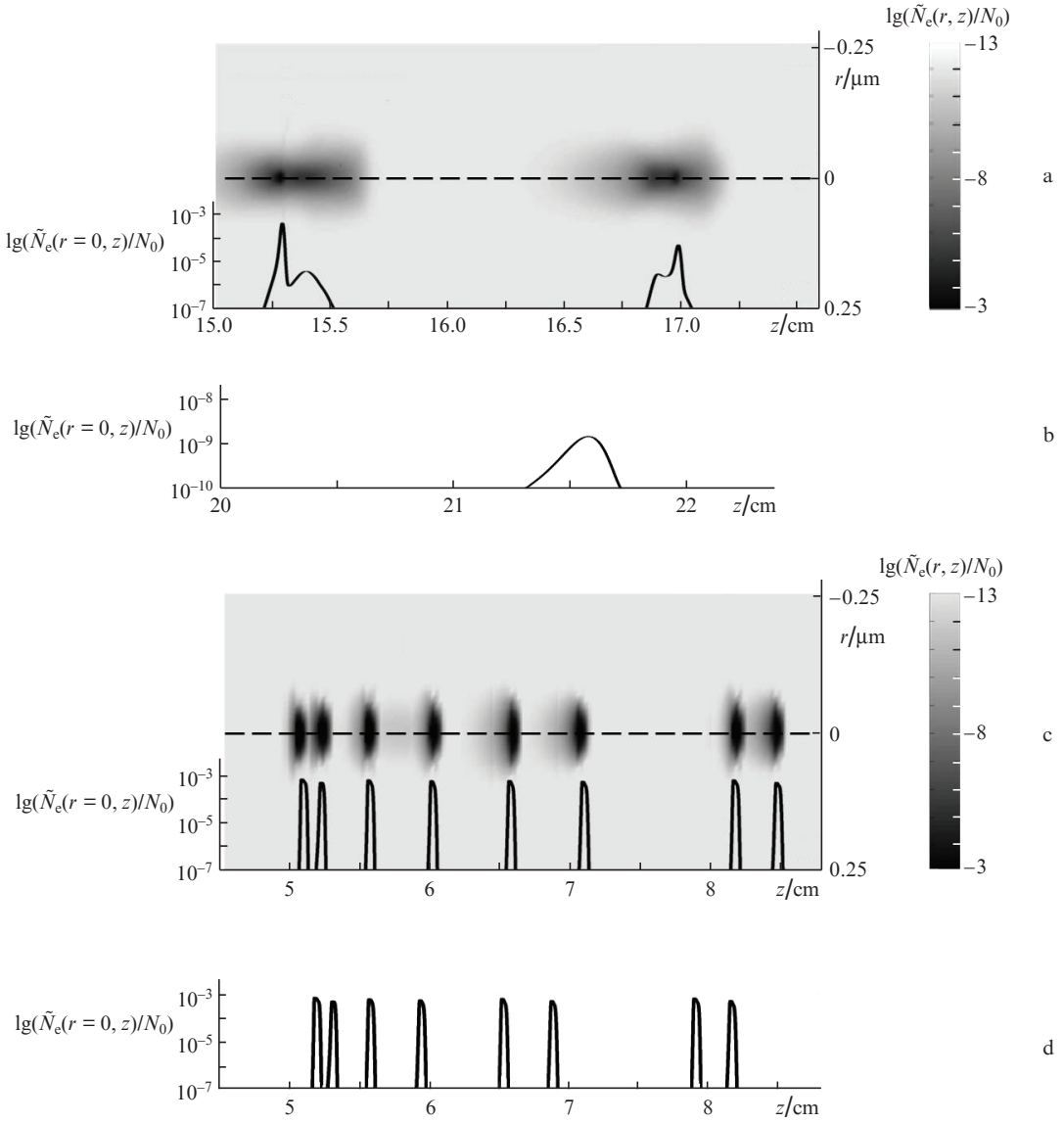

Figure 3. Numerically obtained tone images of (a, c) changes in the radial distribution of electron density, $N_e(r, z)$, with the spacing and the corresponding electron densities along the axis $N_e(r = 0, z)$ in the plasma channels, as well as (b, d) changes in the electron density on the plasma channel axis, $N_e(r = 0, z)$, at wavelengths of (a, b) 800 and (c, d) 1800 nm, beam radii at the entrance face of the axicon equal to (a, b) 0.86 and (c, d) 0.9 mm, energies of (a, b) 7.2 and (c, d) 36 μJ and powers of (a–d) $60P_{cr}$. Axicon focuses light with (a, c) flat and (b, d) divergent ($R \approx 3$ m) wavefronts, the distance z is measured from the entrance face of the sample touching the axicon tip, and the density of neutral atoms is $N_0 = 2.1 \times 10^{28}$ m^{-3}.

beam at $\lambda = 1800$ nm (Fig. 3c), which corresponds to the experimental results (Fig. 2b). In this case, according to the numerical simulation the spacings between the channels change slightly. A monotonic increase in the spacing between plasma channels is observed during filamentation of pulses at a wavelength corresponding to the region of anomalous dispersion under conditions of the lens focusing of a Gaussian beam [18]. However, in the case of axicon focusing the increase in the channel spacing gives way to a decrease, which indicates the role of axicon focusing in the formation of a chain of plasma channels. Indeed, under conditions of anomalous dispersion during filamentation of axicon-focused light, the formation of light bullets is determined not only by temporal compression, but also by an energy transport to the central lobe of the intensity distribution due to the periphery of the beam. With approaching the area of the axicon focus, Z_{Bess}, the contribution of the beam periphery to the increase in the power of the central lobe of the Bessel–Gaussian distribution increases.

Figures 3a and 3b show that the wavefront divergence of the focused radiation with $\lambda = 800$ nm significantly affects the formation of plasma channels. One can see that the defocusing of the constant-energy beam incident on the axicon leads to a decrease in the plasma density in the plasma channel by five or six orders of magnitude, i.e., almost to its disappearance. If during filamentation under conditions of normal group-velocity dispersion a weak divergence of the incident beam can lead to a dramatic change in the filamentation regime, then under conditions of anomalous dispersion it entails only a change in the geometry of the plasma channels. This is due to the fact that the formation of the plasma channel at $\lambda = 1800$ nm is determined by an increasing peak power

of laser pulses in the process of formation of the light bullets, i.e., by a greater pulse temporal dynamics, whereas at $\lambda = 800$ nm, the peak power can be increased only at the expense of the geometric focusing of the beam.

Note that the chain of plasma channels obtained experimentally and numerically during axicon focusing of a beam at wavelengths corresponding to normal and anomalous dispersion is qualitatively different from a continuous extended channel in air, observed in [13] under conditions of normal dispersion. Thus, according to [13], defocusing of the beam incident on the axicon increases the length of the continuous channel, rather than the length of a sequence of plasma formations.

5. Role of the axicon in regularisation of multiple filamentation

For the most extended plasma channels to be obtained in the regime of a single filament, the axicon focusing of a beam with a slightly divergent wavefront has considerable advantages. According to the experimental results obtained in the geometry in question (see Fig. 1), for pulses at $\lambda = 800$ nm the condition of the single-filament regime is met at a pulse energy in the range from 12 μJ (peak power $100P_{cr}$) to 41 μJ (peak power $350P_{cr}$), and at $\lambda = 1800$ nm – at a pulse energy in the range from 15 μJ (peak power $25P_{cr}$) to 105 μJ (peak power $175P_{cr}$). Figure 4 shows the experimentally observed filaments for pulses with an energy that is maximally allowable in the single-filament regime. The range of allowable energies (excess over the critical peak power) is much wider during filamentation at $\lambda = 800$ nm than at 1800 nm. However, the maximum-to-minimum energy ratio at $\lambda = 800$ nm is equal to 3.5, which is lower than at $\lambda = 1800$ nm, where this value amounts to 7. Therefore, to obtain multiple filamentation at $\lambda = 800$ nm, it is necessary to increase the minimum energy by three times only, whereas at $\lambda = 1800$ nm it can be increased by seven times. Thus, for regularising multiple filamentation and producing coaxial plasma channels inside a material using axicon focusing of a divergent beam, laser pulses at $\lambda = 1800$ nm are more preferable than at 800 nm.

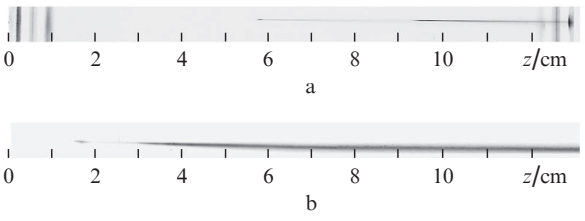

Figure 4. Experimentally observed filaments at the maximum possible (in the single-filament regime) radiation energy at wavelengths of (a) 800 and (b) 1800 nm.

6. Conclusions

In a femtosecond Gaussian beam focused by an axicon, filamentation develops when the peak power of the central lobe of the Bessel–Gaussian intensity distribution exceeds the critical self-focusing power. Changing the wavefront curvature of the Gaussian beam focused by an axicon allows one to control the sequence of coaxial plasma channels formed in the filament due to refocusing. The distance to the start of the plasma channel and the spacing between them in a sequence in a convergent Gaussian beam are smaller than in collimated and divergent beams. With approaching the axicon focus, the spacing between the channels may decrease as a result of the energy influx from the Bessel–Gaussian beam periphery to the filament axis. During filamentation under conditions of normal group-velocity dispersion at $\lambda = 800$ nm, the electron density distribution along the plasma channel is non-unimodal due to the pulse splitting into two or three subpulses with different peak intensities. The length of the plasma channel in this case is 2.8–1.8 mm. Under conditions of anomalous group-velocity dispersion in femtosecond radiation at $\lambda = 1800$ nm, a train of light bullets with a high intensity is produced, which generate plasma channels of length from 0.7 to 0.8 mm; their number in the filament is much greater than in the case of normal dispersion. According to the results of numerical simulation, the peak electron density depends on the wavelength.

In region of high intensity plasma is formed and broadband supercontinuum is generated whose intensity in the visible spectral band decreases with propagation along the filament due to scattering in fused silica and increases again because of its generation in the region of the next plasma channel.

Under conditions of anomalous group-velocity dispersion, the range of laser radiation powers, where the single-filament regime takes place, is much wider than under conditions of normal dispersion.

Acknowledgements. This work was supported by the RF President's Grant Council (State Support to Leading Scientific Schools Programme, Grant No. NSh-3796.2014.2), the Russian Foundation for Basic Research (Grant No. 13-02-90476-Ukr_f_a) and the Presidium of the Russian Academy of Sciences (Extreme Light Fields and Their Applications Programme).

References

1. Durnin J. *J. Opt. Soc. Am. A*, **4**, 445 (1987).
2. McGloin D., Dholakia K. *Contemp. Phys.*, **46**, 15 (2005).
3. Pyatnitskii L.N. *Volnovye besselevy puchki* (Wave Bessel Beams) (Moscow: Fizmatlit, 2012) pp 9, 231.
4. Babin A.A., Kiselev A.M., Pravdenko K.I., Sergeev A.M., Stepanov A.N., Khazanov E.A. *Usp. Fiz. Nauk*, **169**, 80 (1999).
5. Polesana P., Franco M., Couairon A., Faccio D., Di Trapani P. *Phys. Rev. A*, **77**, 043814 (2008).
6. Kompanets V.O., Chekalin S.V., Kosareva O.G., Grigor'evskii A.V., Kandidov V.P. *Kvantovaya Electron.*, **36**, 821 (2006) [*Quantum Electron.*, **36**, 821 (2006)].
7. Xiaodong Sun, Hui Gao, Bin Zeng, Shengqi Xu, Weiwei Liu, Ya Cheng, Zhizhan Xu, Guoguang Mu. *Opt. Lett.*, **37**, 857 (2012).
8. Faccio D., Rubino E., Lotti A., Couairon A., Dubietis A., Tamošauskas G., Papazoglou D.G., Tzortzakis S. *Phys. Rev. A*, **85**, 03389 (2012).
9. Kosareva O.G., Grigor'evskii A.V., Kandidov V.P. *Kvantovaya Electron.*, **35**, 1013 (2005) [*Quantum Electron.*, **35**, 1013 (2005)].
10. Polesana P., Faccio D., Di Trapani P., Dubietis A., Piskarskas A., Couairon A., Porras M. *Opt. Express*, **13**, 6160 (2005).
11. Polynkin P., Kolesik M., Roberts A., Faccio D., Di Trapani P., Moloney J. *Opt. Express*, **16**, 15733 (2008).
12. Akturk S., Zhou B., Franco M., Couairon A., Mysyrowicz A. *Opt. Commun.*, **282**, 129 (2009).
13. Abdollahpour D., Panagiotopoulos P., Turconi M., Jedrkiewicz O., Faccio D., Di Trapani P., Couairon A., Papazoglou D., Tzortzakis S. *Opt. Express*, **17**, 5052 (2009).

14. Chekalin S.V. *Usp. Fiz. Nauk*, **176**, 657 (2006).
15. Smetanina E.O., Dormidonov A.E., Kandidov V.P. *Laser Phys.*, **22**, 1189 (2012).
16. Chekalin S.V., Kandidov V.P. *Usp. Fiz. Nauk*, **183**, 133 (2013).
17. Smetanina E.O., Kompanets V.O., Chekalin S.V., Kandidov V.P. *Kvantovaya Electron.*, **42**, 920 (2012) [*Quantum Electron.*, **42**, 920 (2012)].
18. Smetanina E.O., Kompanets V.O., Chekalin S.V., Kandidov V.P. *Kvantovaya Electron.*, **42**, 913 (2012) [*Quantum Electron.*, **42**, 913 (2012)].